Chemical Physics Letters 585 (2013) 15–20

Contents lists available at ScienceDirect

Chemical Physics Letters

journal homepage: www.elsevier.com/locate/cplett

Sneaking up on the Criegee intermediate from below: Predicted photoelectron spectrum of the CH_2OO^- anion and W3-F12 electron affinity of CH_2OO

A. Karton, M. Kettner, D.A. Wild *

School of Chemistry and Biochemistry, The University of Western Australia, M310, 35 Stirling Hwy, Crawley 6009, Australia

ARTICLE INFO

Article history:
Received 8 July 2013
In final form 17 August 2013
Available online 24 August 2013

ABSTRACT

High level ab initio calculations were undertaken on the CH_2OO anion and neutral species to predict the electron affinity and anion photoelectron spectrum. The electron affinity of CH_2OO, 0.567 eV, and barrier height for dissociation of CH_2OO^- to O^- and CH_2O, 16.5 kJ/mol, are obtained by means of the W3-F12 thermochemical protocol. Two major geometric differences between the anion and neutral, being the dihedral angle of the terminal hydrogen atoms with respect to C–O–O plane, and the O–O bond length, are reflected in the predicted spectrum as pronounced vibrational progressions.

© 2013 Elsevier B.V. All rights reserved.

1. Introduction

Elucidation of the properties and reaction pathways of Criegee intermediates has gained fresh momentum recently. These intermediates, first proposed by Criegee in 1949 [1], are of importance in the ozonolysis and breakdown of unsaturated hydrocarbons, which has been shown to be a major pathway in the troposphere leading to OH radicals and particulate matter [2–4]. The simplest Criegee intermediate is CH_2OO and has in previous work been named formaldehyde oxide, peroxymethylene, or more generally as a carbonyl oxide.

The reason for the renewed activity can be attributed to a breakthrough by Taatjes and co-workers who developed novel gas-phase synthetic techniques for the Criegee intermediates. They first used the Chlorine atom initiated reaction with DMSO, followed by photolysis to form CH_2OO [5], and shortly after a second route was developed whereby they photolysed CH_2I_2 in the presence of O_2 [6]. In this second study, the authors determined rates of reaction between the Criegee intermediate and atmospherically important species NO, NO_2, SO_2, and H_2O.

Since the breakthrough of this new synthetic approach there has been a burst of activity to characterise the Criegee Intermediate by gas phase IR spectroscopy in the 800–1500 cm^{-1} region [7] and determination of the UV absorption cross section and photochemistry [8]. The infrared spectrum was interpreted with the aid of ab initio calculations where three other possible structures for CH_2O_2 were computed, dioxirane, methylenebis(oxy) (also known as dioxymethane), and formic acid, and compared with the experimental spectrum. Clearly the best match between experiment and theory was with the Criegee intermediate, thereby providing definitive proof of its synthesis. Lester and co-workers reported the UV absorption of the CH_2OO biradical in the 320–350 nm region, assigned to the B ← X transition [8], where the excited state (B) is purely repulsive along the O–O coordinate. Results from this work are extremely useful, as they identified the signature of the Criegee intermediate that can be applied in future laboratory or field studies.

The Criegee intermediates have received quite a deal of theoretical attention over the years, with the state of play well represented in references [9], [10], and [11] and references cited therein. Fang et al. studied the potential energy surface of the reaction of CH_2 and O_2 on the singlet and triplet surfaces using CASSCF-type calculations.[9] Nguyen et al. [10] obtained the heat of formation and ionisation energy of the Criegee intermediate at the CCSD(T)/CBS level using W1 theory [12]. It is worthwhile noting that quite recently, Dyke and co-workers used TDDFT, EOM-CCSD, and CASSCF methods to investigate the first few excited electronic states of the simplest CH_2OO intermediate [13]. They also predicted the form of the photoelectron spectrum, i.e. cation ← neutral transitions.

In this contribution, evidence for the stability of the CH_2OO^- anion from high level W3-F12 calculations is provided. The anion is stable with respect to both autodetachment to the CH_2OO neutral and unimolecular dissociation to CH_2O (formaldehyde) and O^- products. We believe that it will be possible to characterise the neutral CH_2OO, and possibly larger, Criegee intermediates through anion photoelectron spectroscopy; a valuable method for mapping

* Corresponding author. Fax: +61 8 6488 1005.
E-mail address: duncan.wild@uwa.edu.au (D.A. Wild).

0009-2614/$ - see front matter © 2013 Elsevier B.V. All rights reserved.
http://dx.doi.org/10.1016/j.cplett.2013.08.075

out the vibrational and electronic states of neutral species. These experiments are appealing as mass spectrometry can be used to isolate the target complex out of an ion population prior to spectroscopic interrogation. Our laboratory has recently made contributions in this area [14–16].

To the best of the authors' knowledge, there have been no previous computational or experimental investigations of the CH_2OO^- anion. A computational study by Roos and co-workers deals with dioxyrane, dioxymethane, and the dioxymethane anion [17], however the dioxymethane species have both oxygen atoms bound to carbon and not to each other, while for dioxyrane there is an O–O bond. There has been experimental work undertaken on very similar species, namely the alkyl peroxides CH_3OO^- and $CH_3CH_2OO^-$. Blanksby et al. produced negative ion photoelectron spectra and determined the adiabatic electron affinities of CH_3OO and CH_3CH_2OO to be (1.161 ± 0.005) eV and (1.154 ± 0.004) eV respectively [18]. The spectrum of the CH_3OO^- anion showed resolved vibrational progressions in the O–O stretching and H_3C-O-O bending modes. The spectrum of the $CH_3CH_2OO^-$ also showed well resolved vibrational progressions. Assignment of one progression to the O–O stretch was clear, while a second progression was assigned to a bending mode; however, it was unclear whether it was the C–C–O or C–O–O mode as these modes are predicted to lie very close in frequency. With regard to the alkyl peroxy systems it would be remiss not to make reference to the work undertaken by Xu et al. [19]. They performed an extensive computational study on the R–OO and R–OO^- anion species with R=CH_3, C_2H_5, n-C_3H_7, n-C_4H_9, n-C_5H_{11}, i-C_3H_7, and t-C_4H_9. They predicted the structures, vibrational frequencies, and electron affinities of the neutral species using seven different density functional or hybrid density functional methods.

In the present Letter we obtain the heat of formation and electron affinity of the Criegee intermediate using the recently developed W3-F12 theory [20]. W3-F12 represents a layered extrapolation to the relativistic, all-electron CCSDT(Q)/CBS energy (complete basis set limit coupled cluster with singles, doubles, triples, and quasiperturbative quadruple excitations) and shows excellent performance for systems containing first-row elements (and H). Specifically, over the 97 first-row systems in the W4-11 dataset [21], W3-F12 attains a root mean square deviation (RMSD) of only 0.88 kJ/mol against all-electron, relativistic reference atomisation energies obtained close to the full configuration interaction (FCI) infinite basis set limit. In addition to the heats of formation and electron affinity of the CH_2OO species, we obtain the barrier height and energy for the $CH_2OO^- \rightarrow CH_2O + O^-$ reaction using W3-F12 theory.

2. Computational methods

The geometries and harmonic frequencies of the anion and neutral CH_2OO species were obtained at the CCSD(T)/A′VQZ level of theory (where A′VnZ indicates the combination of Dunning's aug-cc-pVnZ basis set on carbon and oxygen and the standard cc-pVnZ basis set on hydrogen). The geometry and harmonic frequencies for the transition structure of the $CH_2OO^- \rightarrow CH_2O + O^-$ reaction are obtained at the CCSD(T)/A′VTZ level of theory. The optimised geometries for all the species considered in the present work are given as Cartesian coordinate form in Table S1 of the Supporting information. All the high-level ab initio calculations were performed using the MOLPRO program suite [22], while all the density functional theory (DFT) calculations were carried out with GAUSSIAN 09 [23].

The total atomisation energies at the bottom of the well (TAE_e) of the CH_2OO and CH_2OO^- species are obtained by means of the W3-F12 procedure [20]. W3-F12 theory combines F12 methods [24,25] with extrapolation techniques in order to reproduce the CCSDT(Q) basis set limit energy. The CCSD(T)/CBS energy is obtained from the W2-F12 theory [20] and the post-CCSD(T) contributions are obtained from W3.2 theory [26]. In brief, the Hartree–Fock component is calculated with the VQZ-F12 basis set (VnZ-F12 denotes the cc-pVnZ-F12 basis sets of Peterson et al. which were developed for explicitly correlated calculations) [27]. Note that the complementary auxiliary basis (CABS) singles correction is included in the SCF energy [28–30]. The valence CCSD-F12 correlation energy is extrapolated from the VTZ-F12 and VQZ-F12 basis sets, using the $E(L) = E_\infty + A/L^\alpha$ two-point extrapolation formula, with $\alpha = 3.67$. In all of the explicitly-correlated coupled cluster calculations the diagonal, fixed-amplitude 3C(FIX) ansatz [28,31,32] and the CCSD-F12b approximation [29,33] are employed. The quasiperturbative triples, (T), corrections are obtained from standard CCSD(T) calculations (i.e., without inclusion of F12 terms) and scaled by the factor $f = 0.987 \times E^{MP2\text{-}F12}/E^{MP2}$. This approach has been shown to accelerate the basis set convergence [20,33]. The higher-order connected triples, T_3–(T), valence correlation contribution is extrapolated from the cc-pVDZ and cc-pVTZ basis sets using the above two-point extrapolation formula with $\alpha = 3$, and the parenthetical connected quadruples contribution (CCSDT(Q)–CCSDT) is calculated with the cc-pVDZ basis set [26]. The CCSD inner-shell contribution is calculated with the core-valence weighted correlation-consistent A′PWCVTZ basis set of Peterson and Dunning [34], whilst the (T) inner-shell contribution is calculated with the PWCVTZ(no f) basis set (where A′PWCVTZ indicates the combination of the cc-pVTZ basis set on hydrogen and the aug-cc-pwCVTZ basis set on carbon, and PWCVTZ(no f) indicates the cc-pwCVTZ basis set without the f functions) [20]. The scalar relativistic contribution (in the second-order Douglas–Kroll–Hess approximation [35,36]) is obtained as the difference between non-relativistic CCSD(T)/A′VDZ and relativistic CCSD(T)/A′VDZ-DK calculations (where A′VDZ-DK indicates the combination of the cc-pVDZ-DK basis set on H and aug-cc-pVDZ-DK basis set on C and O) [37]. The atomic spin-orbit coupling terms are taken from the experimental fine structure, and the diagonal Born–Oppenheimer corrections (DBOC) are calculated at the HF/A′VTZ level of theory. The zero-point vibrational energies (ZPVEs) are derived from the harmonic frequencies (calculated at the CCSD(T)/A′VQZ level of theory for the CH_2OO and CH_2OO^- species, and the CCSD(T)/A′VTZ level of theory for the $CH_2O\cdots O^-$ transition structure).

The total atomisation energies at 0 K (TAE_0) are converted to a heats of formation at 298 K using the Active Thermochemical Tables (ATcT) [38–40] atomic heats of formation at 0 K (H 216.034 ± 0.000, C 711.38 ± 0.06, and O 246.844 ± 0.002 kJ/mol), and the CODATA [41] enthalpy functions, H_{298}–H_0, for the elemental reference states ($H_2(g)$ = 8.468 ± 0.001 and C(*cr*,graphite) = 1.050 ± 0.020 kJ/mol), while the enthalpy functions for the CH_2OO and CH_2OO^- species are obtained within the ridged rotor harmonic oscillator (RRHO) approximation from B3LYP/A′VTZ geometries and harmonic frequencies [42–44].

Anion photoelectron spectra were simulated by determining the Franck–Condon Factors (FCFs) linking the anion and neutral CH_2OO species vibrational states. FCFs were calculated using the ezSpectrum 3.0 program which is made freely available by Mozhayskiy and Krylov [45]. The program produces FCFs in either the parallel mode approximation as products of one-dimensional harmonic wavefunctions, or by undertaking Duschinsky rotations of the normal modes between states. Input to the code consists of the output from the ab initio calculations, being geometries, vibrational frequencies, and vibrational normal mode vectors. The predicted stick spectra were convoluted with a Gaussian response function of width 0.002 eV to simulate an experimental spectrum.

3. Results and discussion

3.1. Geometries and vibrational frequencies

The geometry of the neutral Criegee intermediate is well known from previous high level calculations (see Ref. [10] and Refs. cited therein). It has been shown that the C–O and O–O bond lengths are sensitive to the level of theory used is, and it is noted that the values predicted from CCSD(T)/A′VQZ calculations are in line with those reported in Refs. [9] and [10]. Our full data set is provided in Table 1, and a visual comparison of the two species is provided in Figure 1. We predict values of 1.270 Å and 1.343 Å for the C–O and O–O bond lengths respectively, which is in good agreement with the CCSD(T)/AVTZ calculations of Nguyen et al (1.275 Å and 1.349 Å from Ref. [10]). The agreement is also good between our results those from CAS-(8,6)+1+2/cc-pvdz calculations which result in C–O and O–O bond lengths of 1.280 Å and 1.322 Å respectively [9]. Our CCSD(T)/A′VQZ harmonic vibration frequencies are also in good agreement with those reported previously as shown in Table 2.

To the best of our knowledge, the geometry of the analogous Criegee anion, CH_2OO^-, and the geometrical parameters (bond lengths r, bond angles θ, and torsional angles ϕ) at the CCSD(T)/A′VQZ level of theory are presented here for the first time. In essence, the structure of the anion is similar to the neutral, as can be seen in Figure 1, however features longer C–O and O–O bond lengths, increased by 0.064 Å and 0.107 Å respectively. In addition to these two structural differences, the anion species is no longer of C_s symmetry as the hydrogen atoms have moved out of the plane defined by the C–O–O atoms. As presented in Table 1, the H–C–O–O dihedral angles are −17.9° and −164.8° for the Criegee anion, whereas in the neutral species the values are 0° and 180°.

In order to rationalise the differences in anion and neutral geometries we have performed NBO calculations to determine the population of the bonding, anti-bonding, and lone pair natural orbitals [46]. These data, in terms of orbital occupancies, are provided in the Supplementary information. For the anion species increased electron density is predicted in the lone pair orbitals of the carbon, and for the oxygen bound to carbon. The pyramidal nature of the anion complex, compared with the planar neutral, can be rationalised as the population in the carbon lone pair orbital. The NBO calculations also reveal decreased electron density in C–O and O–O bonding orbitals for the anion, leading to the increase in the bond lengths. There is also a marked decrease in the population of the C–O anti-bonding orbital, whereas the O–O anti-bonding orbital occupancy barely changes. This explains the larger change in the O–O bond length compared with the C–O bond length.

Table 1
Computed geometric parameters of the CH_2OO anion and neutral species at the CCSD(T) level of theory, with A′VQZ or A′VTZ basis sets.

	Anion CCSD(T)/A′VQZ	Anion TS CCSD(T)/A′VTZ	Neutral CCSD(T)/A′VQZ
r(C–H) (Å)	1.086, 1.090[a]	1.093, 1.097[a]	1.080, 1.082[a]
r(C–O) (Å)	1.334	1.317	1.270
r(O–O) (Å)	1.450	1.589	1.343
θ(H–C–H) (deg.)	121.1	118.2	126.5
θ(H–C–O) (deg.)	116.4, 113.0[a]	118.2, 119.2[a]	118.7, 114.9[a]
θ(C–O–O) (deg.)	111.7	100.7	117.9
ϕ(H–C–H–O) (deg.)	−145.2, 144.1[a]	−155.9, −156.1[a]	−180.0
ϕ(H–C–O–O) (deg.)	−17.9, −164.8[a]	57.1, −98.8[a]	0.0, 180.0

[a] Where two values are present, the first corresponds to the hydrogen closest to the terminal oxygen.

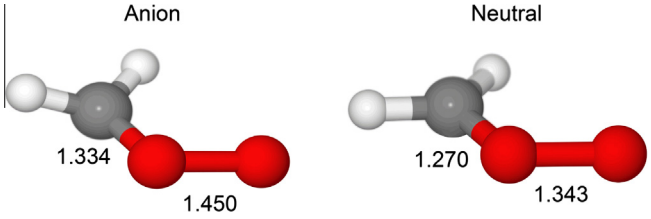

Figure 1. The CH_2OO anion and neutral species. Bond lengths are from CCSD(T)/A′VQZ calculations. Full geometric data are presented in Table 1.

The vibrational modes of the neutral species have been ordered according to the usual numbering scheme appropriate for a C_s symmetry molecule (wavenumber descending in a', and then descending in a'' symmetry). For ease of comparison between the anion and neutral modes, we have adopted the same order for the anion species even though they are all of a symmetry. In any event, the mode description for each mode is provided in the table.

We note that the increased O–O bond length in the anion species is reflected in a reduction of the frequency of the O–O stretching mode, ν_6, from 945 to 776 cm^{-1}, similarly the C–O bond length increase leads to a reduction in vibrational frequency of modes ν_3 and ν_4. The CH_2 wagging mode has also decreased in frequency in the anion species.

3.2. W3-F12 heat of formation and electron affinity of the Criegee intermediate

The components of the W3-F12 total atomisation energies for the CH_2OO and CH_2OO^- species are given in Table 3. At the W2-F12 level, the relativistic, all-electron CCSD(T) contributions to TAE_0 add up to 1520.9 kJ/mol for CH_2OO, and 1581.5 kJ/mol for CH_2OO^-. The TAE_0 for the Criegee intermediate is higher than the W1 value of Nguyen et al. by 1.8 kJ/mol [10]. The lion's share of the difference comes from the valence CCSD(T) components which are closer to the basis set limit in W2-F12 theory (Table S2 of the Supporting information). The reminder of the difference comes mostly from our better geometry and ZPVE and from the DBOC contribution, which is not included in the W1 values.

We now turn our attention to the post-CCSD(T) contributions to the TAE. Table S3 of the Supporting information provides a number of a priori diagnostics for the importance of nondynamical correlation effects, namely the percentage of the total atomisation energy accounted for by the SCF and (T) triples contributions from W3-F12 theory [21,26] (as well as the coupled cluster T_1 and D_1 diagnostics) [47–49]. The CH_2OO neutral and anion species considered in the present study exhibit mild-to-moderate nondynamical correlation effects; 53–55% of the atomisation energy is accounted for at the SCF level, and 3.8–4.6% by the (T) triples. The T_1 diagnostics of above 0.02 (namely, 0.034–0.045) and D_1 diagnostics of above 0.05 (0.122–0.176) also indicate that post-CCSD(T) excitations may have nontrivial contributions. The generally good performance of the CCSD(T)/CBS level of theory in computational thermochemistry can typically be attributed to the large degree of cancellation between higher-order triples contributions, T_3–(T), and post-CCSDT contributions. For systems dominated by dynamical correlation, these contributions are of similar magnitudes, however, the T_3–(T) excitations tend to universally decrease the atomisation energies whereas the post-CCSDT excitations tend to universally increase the atomisation energies. In this regard, we find that for the CH_2OO^- anion there is a significant degree of cancellation between the T_3–(T) contribution (−2.7 kJ/mol) and the (Q) contribution (+4.5 kJ/mol). Resulting in a post-CCSD(T) contribution of 1.8 kJ/mol. However, for the Criegee intermediate there is significantly poorer cancellation between the T_3–(T)

Table 2
Computed vibrational data of the CH_2OO anion and neutral species at the CCSD(T)/A′VQZ level, and comparison with recent published work.

	Anion	Neutral				Mode description
	CCSD(T)/A′VQZ	CCSD(T)/A′VQZ	CCSD(T)/AVTZ	NEVPT2/AVDZ		
				Anh	Har.	
ν_1 (cm^{-1})	3185 a	3302 a′	3290 a′	3370 a′	3149 a′	Asymmetric CH stretch
ν_2 (cm^{-1})	3048 a	3140 a′	3137 a′	3197 a′	3030 a′	Symmetric CH stretch
ν_3 (cm^{-1})	1422 a	1489 a′	1483 a′	1500 a′	1458 a′	CH_2 scissor/CO stretch
ν_4 (cm^{-1})	1252 a	1316 a′	1306 a′	1338 a′	1302 a′	CO stretch/CH_2 scissor
ν_5 (cm^{-1})	1164 a	1239 a′	1231 a′	1235 a′	1220 a′	CH_2 rocking
ν_6 (cm^{-1})	776 a	945 a′	935 a′	916 a′	892 a′	OO stretch
ν_7 (cm^{-1})	466 a	532 a′	529 a′	536 a′	530 a′	COO deformation
[a]ν_8 (cm^{-1})	601 a	876 a″	862 a″	856 a″	853 a″	CH_2 wagging
[a]ν_9 (cm^{-1})	316 a	651 a″	632 a″	620 a″	606 a″	CH_2 twisting
Ref.	This work	This work	[10]	[7]		As in [7]

[a] The ordering of the modes of the anion has been changed to reflect that of the neutral, for direct comparison.

(−3.4 kJ/mol) and (Q) contributions (+9.8 kJ/mol). Therefore, the post-CCSD(T) contributions increase the atomisation energy of CH_2OO by as much as 6.4 kJ/mol. We note that the inclusion of higher-order quadruple contributions, T_4–(Q), is likely to reduce the magnitude of the connected quadruple excitations, and therefore our CCSDT(Q)/CBS values should be regarded as upper limits of the TAEs.

Overall, our best relativistic, all-electron CCSDT(Q)/CBS atomisation energies (Table 3) are 1527.3 (CH_2OO) and 1583.3 (CH_2OO^-) kJ/mol. These correspond to heats of formation at 0 K of 109.9 (CH_2OO) and 53.8 (CH_2OO^-) kJ/mol, and heats of formation at 298 K of 102.8 (CH_2OO) and 48.1 (CH_2OO^-) kJ/mol. In accordance with the large post-CCSD(T) contributions for the Criegee intermediate our W3-F12 heats of formation are lower than the W1 values of Nguyen et al. [10] ($\Delta H_{f,0}$ = 113.0 and $\Delta H_{f,298}$ = 105.9 kJ/mol).

Using the W3-F12 heats of formation for the CH_2OO neutral and anion species electron affinities for the Criegee intermediate of 56.1 kJ/mol at 0 K and 54.7 kJ/mol at 298 K were obtained. It is noted that the post-CCSD(T) contributions to the electron affinity add up to as much as +4.5 kJ/mol.

3.3. Stability of CH_2OO^- with respect to dissociation

In order to determine the stability of the Criegee anion species we modelled the reaction profile for dissociation to the products formaldehyde and oxide. This was achieved by optimising the geometry of the transition state (TS) linking the reactant CH_2OO^- and the products CH_2O and O^- species. The W3-F12 procedure was applied to the TS, anion, and products with the results shown in Figure 2. It is clear that an appreciable barrier to dissociation exists of 16.5 kJ/mol, and therefore should a synthetic route to the anion be found it is likely that it should survive long enough for interrogation.

Table 3
Component breakdown of the W3-F12 total atomisation energies and heats of formation of the CH_2OO neutral and anion species, electron affinity of CH_2OO, and barrier height for the $CH_2OO^- \rightarrow CH_2O + O^-$ reaction (in kJ/mol).

	CH_2OO	CH_2OO^-	EA[a]	BH[b]
SCF	873.4	903.1	29.7	34.0
CCSD	652.0	685.8	33.7	−4.6
(T)	74.4	62.9	−11.5	−5.8
T_3–(T)	−3.4	−2.7	0.8	−1.9
(Q)	9.8	4.5	−5.3	−1.3
Inner-Shell	5.5	5.2	−0.3	0.5
Scalar Relativistic	−1.9	−2.2	−0.3	−0.2
Spin-Orbit	−2.2	−2.2	0.0	0.0
DBOC	0.3	0.1	−0.1	0.1
TAE_e	1608.0	1654.6	46.6	20.7
ZPVE	80.7	71.3	−9.4	4.3
TAE_0	1527.3	1583.3	56.1	16.4
$\Delta H_{f,0}$	109.9	53.8	56.1	16.4
$\Delta H_{f,298}$	102.8	48.1	54.7	16.5

[a] Energy for the $CH_2OO^- \rightarrow CH_2OO + \bar{e}$ reaction.
[b] Barrier height for the $CH_2OO^- \rightarrow CH_2O + O^-$ reaction.

3.4. Predicted anion photoelectron spectrum of CH_2OO^-

Armed with the CCSD(T)/A′VQZ geometries, vibrational frequencies, and normal mode vectors, we are in a position to predict the form of the anion photoelectron spectrum. Therefore the ezSpectrum 3.0 code was employed to simulate the vibronic transitions at a temperature of 10 K, which is appropriate for species entrained in a molecular beam produced via supersonic expansion. Up to 10 quanta were allowed in each excited state vibrational mode (i.e. the modes of the neutral CH_2OO species).

In Figure 3, two stick spectra are presented which are the results from applying the ezSpectrum code with the Duschinsky approach. We also performed simulations using the parallel mode approximation however the differences between the forms of the two predicted spectra were insignificant and do not warrant further discussion. The upper panel of Figure 3 represents a simulation without combination bands included, while the bottom panel is the full predicted spectrum. Data pertaining to these spectra, including predicted line positions, intensities, Franck–Condon

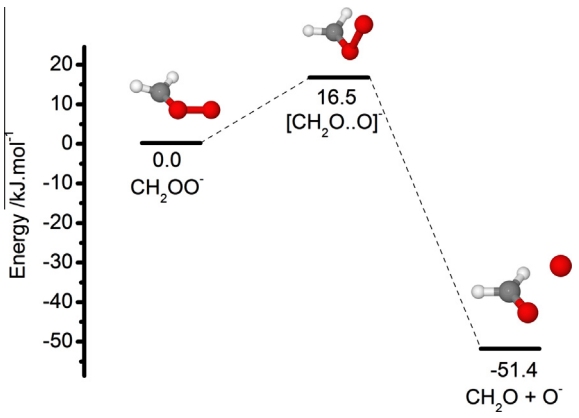

Figure 2. Reaction profile illustrating the dissociation channel of the Criegee anion CH_2OO^- to the products $CH_2O + O^-$ calculated at the W3-F12 level.

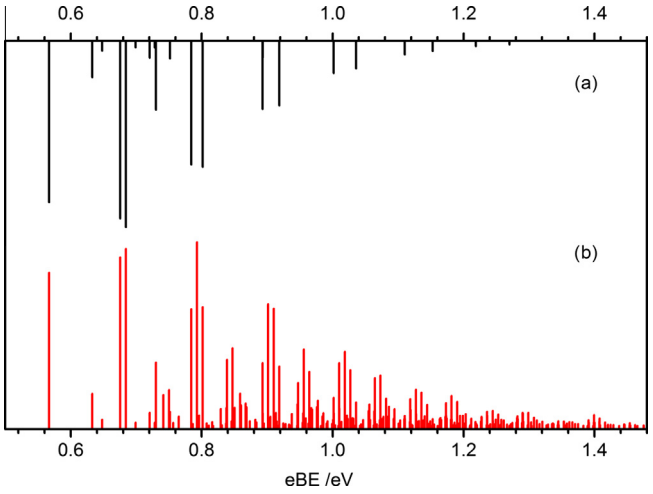

Figure 3. Predicted anion photoelectron stick spectra, (a) no combination bands, (b) with combination bands included.

Factors, and assignments, are provided in the Supplementary information accompanying this Letter.

The major progressions observed in Figure 3a are for the modes ν_6 and ν_8 which correspond to the O–O stretching and CH_2 wagging modes respectively. The fact that these two modes display the longest progressions is consistent with the geometry changes observed between the anion and neutral species. Referring to the data in Table 1, the O–O bond length is predicted to decrease by 0.107 Å, while the two hydrogen atoms move into the C–O–O plane, with the pair of H–C–O–O dihedral angles changing from −17.9° and −164.8° to 0.0° and 180.0°. The low panel of Figure 3 includes the possible combination bands, i.e. those with intensity above the cut off threshold of 0.001 au. The major combination bands are again those associate with the O–O and CH_2 wagging modes. Again, a full list of line positions including assignments is provided in the Supplementary material.

To provide a clearer picture of what an experimental spectrum might look like, we convoluted the line spectrum with a Gaussian response function whose full width at half maximum was set to 0.002 eV and the resulting simulated spectrum is shown in Figure 4. We believe that this is appropriate as this resolution is achievable by the state-of-the-art anion photoelectron spectrometers in use today.

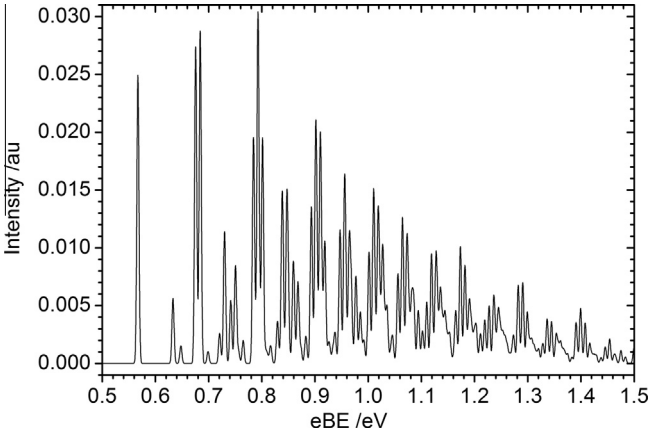

Figure 4. Simulated photoelectron spectrum of CH_2OO^- with the stick spectrum shown in Figure 3b convoluted with Gaussian response function (fwhm = 2 meV).

As a final note, when considering the mass selected photoelectron spectrum of the CH_2OO^- anion one cannot discount the possibility that a van der Waals complex of the form $O^-\ldots CH_2O$ may also be synthesised in addition to the covalently bound CH_2OO^- anion. This possibility needs to be taken into account, however, fortuitously the ionisation energy of the O^- anion is a great deal larger than for CH_2OO^-, with the most recent determination of the electron affinity of the O neutral being 1.439157 eV [50]. The $O^-\ldots CH_2O$ species should be essentially a perturbed O^- anion, due to the weak interaction in a van Der Waals species, and in addition the electron binding energy of the anion generally increases upon formation of a van der Waals complex. Therefore the Criegee anion can be preferentially targeted by selecting a photodetachment photon energy below 1.4 eV.

4. Summary

In summary, we have shown that the CH_2OO^- anion with an analogous structure to the neutral Criegee intermediate exists. The anion is stable with respect to dissociation of the O–O bond, with a barrier of 16.5 kJ/mol, and the electron is bound by 0.567 eV. The major geometric differences between the anion and neutral are in the increased O–O bond length, and the movement of the terminal hydrogen atoms into the plane formed by the C–O–O atoms. Progressions involving both of these modes are prominent in the predicted photoelectron spectrum.

Acknowledgements

We gratefully acknowledge funding (to A.K.) from the Australian Research Council (Discovery Project Grant: DP110102336) and the generous allocation of computing time from the National Computational Infrastructure (NCI) National Facility.

Appendix A. Supplementary data

Supplementary data associated with this article can be found, in the online version, at http://dx.doi.org/10.1016/j.cplett.2013.08.075.

References

[1] R. Criegee, G. Wenner, Chem. Ber. 564 (1949) 9.
[2] D. Johnson, G. Marston, Chem. Soc. Rev. 37 (2008) 699.
[3] R. Gutbrod, R.N. Schindler, E. Kraka, D. Cremer, Chem. Phys. Lett. 252 (1996) 221.
[4] R. Gutbrod, E. Kraka, R.N. Schindler, D. Cremer, J. Am. Chem. Soc. 119 (1997) 7330.
[5] C.A. Taatjes, G.M. Meloni, T.M. Selby, A.J. Trevitt, D.L. Osborn, C.J. Percival, D.E. Shallcross, J. Am. Chem. Soc. 130 (2008) 11883.
[6] O. Welz, J.D. Savee, D.L. Osborn, S.S. Vasu, C.J. Percival, D.E. Shallcross, C.A. Taatjes, Science 335 (2012) 204.
[7] Y.-T. Su, Y.-H. Huang, H.A. Witek, Y.-P. Lee, Science 340 (2013) 174.
[8] J.M. Beames, F. Liu, L. Lu, M.I. Lester, J. Am. Chem. Soc. 134 (2012) 20045.
[9] D.-C. Fang, X.-Y. Fu, J. Phys. Chem. A 106 (2002) 2988.
[10] M.T. Nguyen, T.L. Nguyen, V.T. Ngan, H.M.T. Nguyen, Chem. Phys. Lett. 448 (2007) 183.
[11] L. Vereecken, J.S. Francisco, Chem. Soc. Rev. 41 (2012) 6259.
[12] J.M.L. Martin, G.J. Oliveira, J. Chem. Phys. 111 (1999) 1843.
[13] P.F.E. Lee, D.K.W. Mok, D.E. Shallcross, C.J. Percival, D.L. Osborn, C.A. Taatjes, J.M. Dyke, Chem. Eur. J. 18 (2012) 12411.
[14] K.M. Lapere, R.J. LaMacchia, L.H. Quak, A.J. McKinley, D.A. Wild, Chem. Phys. Lett. 504 (2011) 13.
[15] K.M. Lapere, R.J. LaMacchia, L.H. Quak, M. Kettner, S.G. Dale, A.J. McKinley, D.A. Wild, J. Phys. Chem. A 116 (2012) 3577.
[16] K.M. Lapere, R.J. LaMacchia, L.H. Quak, M. Kettner, S.G. Dale, A.J. McKinley, D.A. Wild, Aust. J. Chem. 65 (2012) 457.
[17] M. Cantos, M. Merchán, F. Tomás-Vert, B. Roos, Chem. Phys. Lett. 229 (1994) 181.
[18] S.J. Blanksby et al., J. Am. Chem. Soc. 123 (2001) 9585.
[19] W. Xu, L. Gaoyu, J. Phys. Chem. A 112 (2008) 6999.
[20] A. Karton, J.M.L. Martin, J. Chem. Phys. 136 (2012) 124114.
[21] A. Karton, S. Daon, J.M.L. Martin, Chem. Phys. Lett. 510 (2011) 165.

[22] H.-J. Werner, et al., MOLPRO, a package of ab initio programs, 2010.
[23] M.J. Frisch et al., GAUSSIAN 09, Gaussian, Inc., Wallingford CT, 2009.
[24] K.A. Peterson, D. Feller, D.A. Dixon, Theor. Chem. Acc. 131 (2012) 1079.
[25] S. Ten-no, J. Noga, WIREs Comput. Mol. Sci. 2 (2012) 114.
[26] A. Karton, E. Rabinovich, J.M.L. Martin, B.J. Ruscic, J. Chem. Phys. 125 (2006) 144108.
[27] K.A. Peterson, T.B. Adler, H.-J. Werner, J. Chem. Phys. 128 (2008) 084102.
[28] G. Knizia, H.-J. Werner, J. Chem. Phys. 128 (2008) 154103.
[29] T.B. Adler, G. Knizia, H.-J. Werner, J. Chem. Phys. 127 (2007) 221106.
[30] J. Noga, S. Kedžuch, J. Šimunek, J. Chem. Phys. 127 (2007) 034106.
[31] S. Ten-no, Chem. Phys. Lett. 398 (2004) 56.
[32] H.-J. Werner, T.B. Adler, F.R. Manby, J. Chem. Phys. 126 (2007) 164102.
[33] G. Knizia, T.B. Adler, H.-J. Werner, J. Chem. Phys. 130 (2009) 054104.
[34] K.A. Peterson, T.H. Dunning, J. Chem. Phys. 117 (2002) 10548.
[35] M. Douglas, N.M. Kroll, Ann. Phys. 82 (1974) 89.
[36] B.A. Hess, Phys. Rev. A 33 (1986) 3742.
[37] W.A. de Jong, R.J. Harrison, D.A. Dixon, J. Chem. Phys. 114 (2001) 48.
[38] B.J. Ruscic et al., J. Phys. Chem. A 108 (2004) 9979.
[39] W.R. Stevens, B.J. Ruscic, T. Baer, J. Phys. Chem. A 114 (2010) 13134.
[40] B.J. Ruscic, R.E. Pinzon, M.L. Morton, N.K. Srinivasan, M.C. Su, J.W. Sutherland, J.V. Michael, J. Phys. Chem. A 110 (2006) 6592.
[41] J.D. Cox, D.D. Wagman, V.A. Medvedev, CODATA Key Values for Thermodynamics, H.P. Corp., New York, 1989.
[42] A.D. Becke, J. Chem. Phys. 98 (1993) 5648.
[43] P.J. Stephens, F.J. Devlin, C.F. Chabalowski, M.J. Frisch, J. Phys. Chem. 98 (1994) 11623.
[44] C. Lee, W. Yang, R.G. Parr, Phys. Rev. B 37 (1988) 785.
[45] V.A. Mozhayskiy, A.I. Krylov, ezSpectrum, http://iopenshell.usc.edu/downloads, 2009.
[46] E.D. Glendening, NBO 6.0 Program, Theoretical Chemistry Institute, University of Wisconsin, Madison, 2013.
[47] T.J. Lee, Chem. Phys. Lett. 372 (2003) 362.
[48] M.L. Leininger, I.M.B. Nielsen, T.D. Crawford, C.L. Janssen, Chem. Phys. Lett. 328 (2000) 431.
[49] T.J. Lee, J.E. Rice, G.E. Scuseria, H.F. Schaefer III, Theor. Chim. Acta 75 (1989) 81.
[50] A. Joiner, R.H. Mohr, J.N. Yukich, Phys. Rev. A 83 (2011) 035401.